Research Article

Received: 1 February 2011 Revised: 27 May 2011 Accepted: 20 July 2011 Published online in Wiley Online Library: 18 November 2011

(wileyonlinelibrary.com) DOI 10.1002/jsfa.4723

Hepatoprotection of silymarin against thioacetamide-induced chronic liver fibrosis

I-Shu Chen,[a†] Yi-Chen Chen,[b†] Chung-Hsi Chou,[c] Ruei-Feng Chuang,[b] Lee-Yan Sheen[d] and Chih-Hsien Chiu[b*]

Abstract

BACKGROUND: Liver fibrosis is chronic liver damage usually caused by alcohol, viruses or other toxins and is characterised by an excessive accumulation of extracellular matrix proteins such as collagen. The aim of this study was to establish an animal model of chronic liver damage and investigate molecular mechanisms of silymarin hepatoprotective effects.

RESULTS: Thioacetamide (TAA; 100 mg kg^{-1} intraperitoneal (i.p.) injection three times weekly) effectively induced chronic liver fibrosis in male ICR mice. Then 24 ICR mice were randomly divided into four groups: (1) saline (i.p.) + water (gavage); (2) saline (i.p.) + 150 mg kg^{-1} silymarin (gavage); (3) 100 mg kg^{-1} TAA (i.p.) + water (gavage); (4) 100 mg kg^{-1} TAA (i.p.) + 150 mg kg^{-1} silymarin (gavage). Eight weeks of TAA treatment resulted in lower body weight, serum cholesterol and triglycerides as well as increased liver size, ALT, AST and LDH values ($P < 0.05$). These TAA-induced effects were attenuated by silymarin ($P < 0.05$); therefore silymarin also ameliorated TAA-induced liver lesions. Effects of silymarin on TAA-induced chronic liver damage may be attributed to down-regulation of hepatic MMP-2, MMP-13, TIMP-1, TIMP-2, AP-1, KLF6, TGF-β1, α-SMA and COL-α1.

CONCLUSION: A mouse model of chronic liver fibrosis was successfully established by injecting 100 mg kg^{-1} TAA three times weekly in male ICR mice. Meanwhile, silymarin showed hepatoprotection against TAA-induced damage.

Keywords: thioacetamide; chronic liver fibrosis; silymarin; MMP/TIMP families; hepatic stellate cell activation

INTRODUCTION

The International Agency for Research on Cancer reported in 2009 that liver cancer is the third leading cause of cancer-related deaths in men and the eighth leading cause in women worldwide.[1] Similarly, liver cancer was ranked second for cancer-related deaths in Taiwan in 2008.[2] Liver cancer is highly related to chronic liver diseases (i.e. liver fibrosis, cirrhosis, hepatitis and steatohepatitis).[3] Liver fibrosis is chronic liver damage usually caused by alcohol, viruses or other toxins and is characterised by an excessive accumulation of extracellular matrix (ECM) proteins such as collagen.[4] The injured liver cells stimulate hepatic stellate cells to transform into myofibroblast-like cells, which secrete large amount of collagen, thereby producing liver fibrosis. The goal of food scientists and nutritionists is to reduce liver fibrogenesis by decreasing ECM degradation and normalising hepatic stellate cell activation via dietary intervention.

The hepatotoxin thioacetamide ($CH_3C(S)NH_2$, TAA) was first used to control the decay of oranges and has subsequently been used as a fungicide.[5] Although TAA itself is not toxic to the liver, its intermediates (i.e. thioacetamide-*S*-oxide and thioacetamide-*S*,*S*-dioxide via the cytochrome P450 (CYP2E1) and/or flavin-containing monooxygenase (FMO) systems) are able to covalently bind to hepatic macromolecules and eventually initiate necrosis of liver cells.[6] Hence TAA is widely used to induce acute and chronic liver disease.[7–9] Further, the TAA intermediate thioacetamide-*S*-oxide is a reactive oxygen species that further damages the liver during detoxification of TAA.[10]

Antioxidants and free radical-scavenging compounds have been reported to alleviate liver damage related to oxidative stress.[7,11] Silymarin extracted from the milk thistle (*Silybum marianum*) is composed of the flavonoids silybin, silydianin and silychristin and is well regarded for its antioxidant and chemoprotective effects on the liver.[12] Saller *et al.*[13] demonstrated that silymarin exerts hepatoprotective effects against alcohol-induced oxidative stress. Silymarin has also been shown to protect the kidney against acetaminophen damage[14] and the liver against carbon tetrachloride (CCl_4) damage,[15] effects primarily attributed to reduced lipid peroxidation.

Liver fibrosis can also be caused by recurrent wound healing in response to chronic inflammation and ECM remodelling.

* *Correspondence to: Chih-Hsien Chiu, Department of Animal Science and Technology, National Taiwan University, Taipei 106, Taiwan. E-mail: chiuchihhsien@ntu.edu.tw*

† *I-Shu Chen and Yi-Chen Chen contributed equally to this study as co-first authors.*

a *Department of Surgery, Veteran General Hospital, Kaohsiung, Taiwan*

b *Department of Animal Science and Technology, National Taiwan University, Taipei 106, Taiwan*

c *School of Veterinary Medicine, National Taiwan University, Taipei 106, Taiwan*

d *Institute of Food Science and Technology, National Taiwan University, Taipei 106, Taiwan*

Matrix metalloproteinases (MMPs) are a family of zinc-dependent proteinases that play a central role in ECM degradation and remodelling.[16] MMP inhibitors (tissue inhibitors of metalloproteinases, TIMPs) not only inhibit MMP activity but also modulate MMP function. Therefore, when various protease systems are activated in response to tissue damage, a corresponding increase in protease inhibitor molecules occurs as well.[17] Lichtinghagen *et al.*[18] observed that levels of MMP-2, MMP-7 and MMP-9 as well as TIMP-1 and TIMP-2 increase during hepatitis C virus-induced end-stage cirrhosis.

Activation of hepatic stellate cells (HSCs) is also regarded as a major cause of liver fibrosis. Several transcriptional factors, including nuclear factor kappa light chain enhancer of activated B cells (NF-κB), activator protein 1 (AP-1) and Kruppel-like factor 6 (KLF6), are associated with HSC activation. HSC activation generates the alpha smooth muscle actin (α-SMA)-positive myofibroblast-like cells that are responsible for scar tissue formation in the fibrotic liver.[19] A recent report indicated that KLF6 regulates several profibrogenic genes expressed in activated HSCs, such as transforming growth factor beta 1 (TGF-β1) and collagen alpha 1 (COL-α1).[20]

The aim of the present study was to establish an animal model of chronic liver fibrosis and then characterise the molecular mechanism of silymarin protection against chronic liver fibrosis by evaluating serum markers of liver damage and liver histopathology.

MATERIALS AND METHODS

Animals and treatments

Animal use and protocols were reviewed and approved by the National Taiwan University Institutional Animal Care and Use Committee. Chia *et al.*[21] reported that, owing to the difference in genetic variation between inbred and outbred strains, outbred mouse stocks are more suitable for toxicology and pharmacology research because of their similarity to the human population. On the other hand, rats and mice do not belong to the same genus, so their responses to a particular treatment might differ. Moreover, for economic and convenience-of-handling reasons, mice are a better choice than rats. Hence a total of 66 male ICR mice (outbred strain) weighing between 25 and 30 g were purchased from BioLASCO Taiwan Co., Ltd (Taipei, Taiwan). The mice were housed in one cage in an animal room at 22±2 °C with a 12/12 h light/dark cycle. Mouse chow containing 487 g carbohydrate, 239 g protein, 50 g fat, 51 g fibre and 70 g ash kg^{-1} (Laboratory Rodent Diet 5001, PMI® Nutrition International/Purina Mills LLC, Richmond, IN 47374, USA) and water were provided *ad libitum*. All mice were acclimatised for 1 week prior to the beginning of all experiments. TAA was purchased from Sigma Aldrich (St Louis, MO, USA) and dissolved in sterile saline. This study was divided into two experiments.

Development of a mouse model of chronic liver fibrosis

Based on a literature search, no exact TAA dosage and applied method to introduce chronic liver fibrosis were available, e.g. 300 mg kg^{-1} body weight (BW) in drinking water[22] or 200 mg kg^{-1} BW.[23,24] Hence, 30 male ICR mice were randomly divided into five groups ($n = 6$ per group). To determine the appropriate dosage of TAA to induce chronic liver fibrosis, the groups of mice were subjected to intraperitoneal (i.p.) injection with 0 (sterile saline only), 100, 200, 400 or 600 mg TAA kg^{-1} BW once daily for three consecutive days. After 1 week of observation, 100% of mice survived in only two groups: the 0 and 100 mg TAA kg^{-1} treatment groups. Therefore a dose of 100 mg kg^{-1} was chosen to establish the animal model of chronic liver fibrosis. Next, 12 male ICR mice were randomly divided into two groups ($n = 6$ per group). One group received an i.p. injection of sterile saline (control group) and the other received 100 mg kg^{-1} TAA (TAA group). Injections were administered three times weekly (Monday, Wednesday and Friday) for 8 weeks, after which analysis of serum biochemistry and liver histopathology was performed to confirm chronic liver fibrosis.

Determination of molecular mechanism of silymarin action in chronic liver fibrosis

Twenty-four male ICR mice were randomly divided into four groups: (1) saline (i.p.) + doubly distilled water (ddH_2O; gavage); (2) saline (i.p.) + 150 mg kg^{-1} silymarin (gavage); (3) 100 mg kg^{-1} TAA (i.p.) + ddH_2O (gavage); (4) 100 mg kg^{-1} TAA (i.p.) + 150 mg kg^{-1} silymarin (gavage). For 8 weeks the saline or TAA injections were administered on Monday, Wednesday and Friday and the ddH_2O or silymarin oral gavages on Tuesday, Thursday and Saturday. Body weight, liver size, serum biochemical values and histopathological results were analysed at the end of the 8 week experiment.

Serum and liver specimens and determination of serum biochemical values

At the end of all experiments the mice fasted overnight. They were then euthanised by CO_2, after which the liver from each mouse was removed and weighed. Blood samples were obtained by intracardiac puncture. Serum was separated from blood samples by centrifugation at 3000 × *g* for 10 min and then stored at −80 °C for subsequent analyses. Serum glucose, total cholesterol (T-cholesterol), total triglyceride (T-triglyceride), blood urea nitrogen (BUN), total bilirubin (T-bilirubin), total protein (T-protein), calcium (Ca), uric acid, aspartate aminotransferase (AST), alanine aminotransferase (ALT) and lactate dehydrogenase (LDH) were determined using commercial enzymatic kits with a SPOTCHEM™ EZ SP-4430 biochemistry analyser (ARKRAY, Inc., Kyoto, Japan).

Histopathological examination

The liver tissues were fixed in neutral-buffered formalin solution for no more than 24 h, dehydrated in graded alcohol, cleared in xylene and then embedded in paraffin. Histopathological examination was performed by haematoxylin and eosin (H&E) and Masson's Trichrome staining. A METAVIR fibrosis score from 0 to 4 was used to differentiate the levels of liver fibrosis. Score 0 indicates no liver scarring. Score 1 indicates minimal liver scarring around the liver portal tract but without septa formation. Score 2 indicates an enlargement of the portal tract with rare septa formation. Score 3 indicates numerous septa without cirrhosis. Score 4 indicates extensive scarring or cirrhosis.[25]

Expression of hepatic MMP and TIMP gene families, hepatic stellate cell activation and profibrosis

Total RNA was isolated from the frozen liver tissue with RNeasy Mini Kits (Qiagen, Valencia, CA, USA) according to the manufacturer's instructions. Reverse transcription was carried out with 2 µg of total RNA, 8 µL of reaction buffer, 2 µL of dNTPs, 4.8 µL of $MgCl_2$, 4 µL of oligo-dT (10 µmol L^{-1}), 200 U of reverse transcriptase (Promega,

Madison, WI, USA) and diethyl pyrocarbonate (DEPC) water to reach a final volume of 40 μL; reactions were incubated at 42 °C for 1 h. After heat inactivation, 1 μL of cDNA product was used as template for polymerase chain reaction (PCR) amplification. The primers for target genes were designed for mouse MMP-2 (GenBank No. NM_008 610), MMP-8 (GenBank No. NM_008 611), MMP-9 (GenBank No. NM_013 599.2), MMP-13 (GenBank No. NM_008 607), TIMP-1 (GenBank No. NM_011 593.3), TIMP-2 (GenBank No. NM_011 594), NF-κB (GenBank No. NM_008 689.2), AP-1 (GenBank No. NM_010 591.2), KLF6 (GenBank No. NM_011 803.2), TGF-β1 (GenBank No. NM_011 577), α-SMA (GenBank No. NM_001 613), COL-α1 (GenBank No. BC003198) and β-actin (GenBank No. NM_007 393.2) as follows: MMP-2 sense 5′-CAC ACC AGG TGA AGG ATG TG-3′, antisense 5′-GCC CTC CTA AGC CAG TCT CT-3′; MMP-8 sense 5′-AAC GGT CTT CAG GCT GCT TA-3′, antisense 5′-GGG AAC ATG CTT GGT ATG CT-3′; MMP-9 sense 5′-CGA CAG CAC CTC CCA CTA TG-3′, antisense 5′-CCC AAC TTA TCC AGA CTC CT-3′; MMP-13 sense 5′-CCT GGA ATT GGC AAC AAA GT-3′, antisense 5′-TAG CAC GCA AGA ATC AGG TG-3′; TIMP-1 sense 5′-TCC CCA GAA ATC AAC GAG AC-3′, antisense 5′-CTC AGA GTA CGC CAG GGA AC-3′; TIMP-2 sense 5′-TCC TTG CTA CAG GCA GGA GT-3′, antisense 5′-CAT TCG CTG AAG TCT GTG GA-3′; NF-κB sense 5′-CAT GAA GCA GCT GAC AGA AG-3′, antisense 5′-TTC AAT AGG TCC TTC CTG CC-3′; AP-1 sense 5′-CCG AGA GCG GTG CCT ACG GCT ACA G-3′, antisense 5′-GAC CGG CTG TGC CGC GGA GGT GAC-3′; KLF6 sense 5′-TGT AGC ATC TTC CAG GAA CTA CAG A-3′, antisense 5′-TGA CAC GTA GCA GGG CTC ACT-3′; TGF-β1 sense 5′-CTA ATG GTG GAC CGC AAC AAC-3′, antisense 5′-CGG TTC ATG TCA TGG ATG GTG-3′; α-SMA sense 5′-CCG ACC GAA TGC AGA AGG A-3′, antisense 5′-ACA GAG TAT TTG CGC TCC GGA-3′; COL-α1 sense 5′-TTC ACC TAC AGC ACC CTT GT-3′, antisense 5′-TCT TGG TGG TTT TGT ATT CGA TGA-3′; β-actin sense 5′-TGT TAC CAA CTG GGA CGA CA-3′, antisense 5′-TCT CAG CTG TGG TGG TGA AG-3′. The amplicon sizes were as follows: MMP-2, 307 bp; MMP-8, 275 bp; MMP-9, 481 bp; MMP-13, 376 bp; TIMP-1, 251 bp; TIMP-2, 386 bp; NF-κB, 496 bp; AP-1, 350 bp; KLF6, 135 bp; TGF-β1, 431 bp; α-SMA, 88 bp; COL-α1, 85 bp; β-actin, 394 bp.

PCR amplification was carried out using a GeneAmp® PCR System 9700 (Applied Biotechnology, Inc., Foster City, CA, USA) under the following conditions: MMP-2 and MMP-13: 40 cycles at 94 °C for 20 s, 57 °C for 1 min and 72 °C for 1 min followed by 10 min at 72 °C; MMP-9: 40 cycles at 94 °C for 20 s, 56 °C for 1 min and 72 °C for 1 min followed by 10 min at 72 °C; MMP-8, TIMP-1 and TIMP-2: 39 cycles at 94 °C for 20 s, 57 °C for 1 min and 72 °C for 1 min followed by 10 min at 72 °C; AP-1: 38 cycles at 94 °C for 20 s, 57 °C for 1 min and 72 °C for 1 min followed by 10 min at 72 °C; NF-κB: 36 cycles at 94 °C for 20 s, 57 °C for 1 min and 72 °C for 1 min followed by 10 min at 72 °C; KLF6 and TGF-β1: 34 cycles at 94 °C for 20 s, 57 °C for 1 min and 72 °C for 1 min followed by 10 min at 72 °C; α-SMA, COL-α1 and β-actin: 33 cycles at 94 °C for 20 s, 58 °C for 1 min and 72 °C for 1 min followed by 10 min at 72 °C. The final products were subjected to 20 g kg^{-1} agarose gel electrophoresis and ethidium bromide staining, then visualised by UV light. The relative expressions of the target genes were normalised using β-actin as an internal standard.

Statistical analysis

In the first experiment, statistical analyses of data were performed using Student's *t* test. The second experiment was conducted using a 2 × 2 factorial arrangement of treatment design. The interaction effect (TAA × silymarin) and main effect (TAA and silymarin) were analysed. All significant differences in the interaction effect and main effect were tested using analysis of variance (ANOVA) at 0.05 probability level. When a significant difference in the interaction effect was obtained, the least significant difference (LSD) test at 0.05 probability level was used to test differences between combination treatments. All statistical analyses of data were performed using SAS (SAS Institute, Cary, NC, USA).

Table 1. Effects of 8 weeks of thioacetamide (TAA) treatment on relative liver size and serum biochemical values in male ICR mice

Parameter	Control	TAA
Liver size (g per100 g body weight)	4.0 ± 0.4	6.2 ± 0.5*
Glucose (mg dL^{-1})	156.2 ± 19.5*	110.7 ± 17.0
T-cholesterol (mg dL^{-1})	161.0 ± 16.5*	109.7 ± 22.4
T-triglyceride (mg dL^{-1})	79.2 ± 15.5*	63.2 ± 9.5
BUN (mg dL^{-1})	30.3 ± 5.7	32.2 ± 6.1
T-bilirubin (mg dL^{-1})	0.2 ± 0.1	0.2 ± 0.0
T-protein (g dL^{-1})	5.9 ± 0.5	5.7 ± 0.4
Albumin (g dL^{-1})	3.3 ± 0.3	3.6 ± 0.5
Ca (mg dL^{-1})	10.2 ± 0.6	10.4 ± 0.4
Uric acid (mg dL^{-1})	4.2 ± 1.2	4.7 ± 1.1
AST (IU L^{-1})	101.8 ± 20.5	137.4 ± 24.7*
ALT (IU L^{-1})	40.7 ± 10.3	109.5 ± 14.9*
LDH (IU L^{-1})	1394.3 ± 270.9	2014.8 ± 385.5*

Data are expressed as mean ± standard deviation ($n = 6$). * $P < 0.05$. T-cholesterol, total cholesterol; T-triglyceride, total triglyceride; BUN, blood urea nitrogen; T-bilirubin, total bilirubin; T-protein, total protein; Ca, calcium; AST, aspartate aminotransferase; ALT, alanine aminotransferase; LDH, lactate dehydrogenase.

RESULTS

Establishment of an animal model of chronic liver fibrosis with TAA

A range of TAA concentrations were tested to determine the appropriate dosage for induction of chronic liver fibrosis in male ICR mice. One-week survival rates were 100% (0% TAA; sterile saline), 100% (100 mg kg^{-1} TAA), 66.7% (200 mg kg^{-1} TAA), 0% (400 mg kg^{-1} TAA) and 0% (600 mg kg^{-1} TAA). This result indicated that 100 mg kg^{-1} TAA does not induce acute lethality in male ICR mice. Serum biochemical values and liver histopathology were assessed in mice injected with sterile saline and 100 mg kg^{-1} TAA (Table 1 and Fig. 1). Mice receiving TAA had significantly larger livers and increased AST, ALT and LDH levels ($P < 0.05$) but significantly lower serum glucose, T-cholesterol and T-triglyceride levels compared with the control group ($P < 0.05$). As for the histopathology exam, H&E staining revealed that TAA treatment caused acute focal necrosis and vacuolisation in some liver cells, with mild inflammatory cell infiltration (Fig. 1(A)). Masson's Trichrome stain was used to detect collagen distribution in the liver to estimate the level of liver fibrosis. Livers from TAA-treated mice showed apparent collagen deposition between liver lobules (Fig. 1(B)). In comparison with the control group, TAA treatment led to a higher METAVIR fibrosis score (2.17), which means an enlargement of the portal tract with rare septa formation (Fig. 1(C)).

Protective molecular mechanism of silymarin on TAA-induced chronic liver fibrosis

Eight weeks of treatment with silymarin alone did not affect body weight or liver size (Fig. 2) or alter serum biochemical values

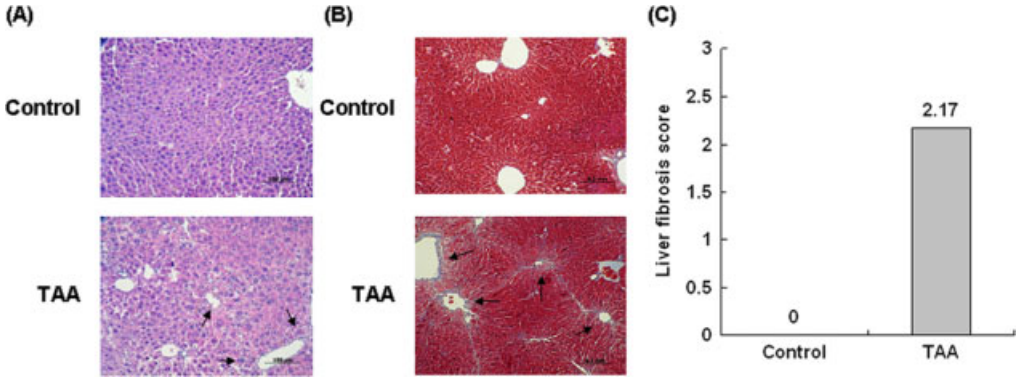

Figure 1. Histopathological analysis of mouse livers after 8 weeks of thioacetamide (TAA) treatment. (A) H&E stain revealed acute focal necrosis and vacuolisation with mild inflammatory cell infiltration (arrows). (B) Masson's Trichrome stain showed collagen deposition between liver lobules (arrows). (C) METAVIR fibrosis scores.

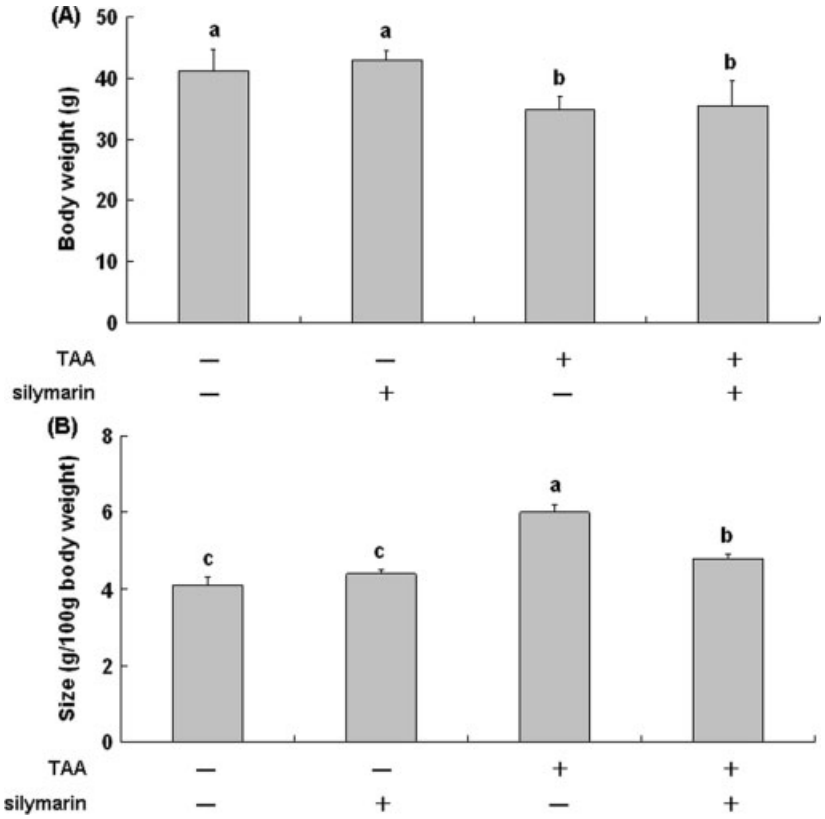

Figure 2. Silymarin attenuated some effects of 8 weeks of thioacetamide (TAA) treatment in male ICR mice. (A) Body weight was reduced by TAA but was unaffected by co-treatment with silymarin. (B) Relative liver size was increased by TAA, but this effect was attenuated by silymarin. Data are expressed as mean ± standard error of mean ($n = 6$). Different letters indicate significant differences ($P < 0.05$).

compared with saline. TAA treatment resulted in significantly lower body weight and increased liver size compared with control treatment, which was consistent with results from the first experiment. Co-treatment with silymarin attenuated the increased liver size of TAA-injured mice ($P < 0.05$) (Fig. 2(B)). TAA dramatically increased AST, ALT and LDH levels ($P < 0.05$) and reduced T-cholesterol and T-triglyceride levels; these effects were also attenuated by silymarin ($P < 0.05$), except for T-cholesterol (Table 2). Mice injected with sterile saline showed liver lobules without pathological lesions (Figs 3(A) and 3(B)). In contrast, 8 weeks of TAA treatment resulted in acute focal necrosis and vacuolisation in some liver cells, with mild inflammatory cell infiltration. Lobular damage and collagen deposition between liver lobules were also observed in TAA-treated mice; however, fewer liver lesions were observed in TAA-treated mice that also received silymarin. Corresponding results were also demonstrated in the METAVIR fibrosis scores, where higher scores were given in TAA-treated mice, but a decreased score was obtained in TAA-treated mice receiving silymarin (Fig. 3(C)).

To elucidate the mechanism of silymarin action, expression of hepatic MMP and TIMP gene families as well as genes involved in HSC activation and profibrosis was evaluated. As shown in Fig. 4, 8 weeks of treatment with silymarin alone did not alter gene expression of MMPs or TIMPs compared with

Table 2. Effects of silymarin on serum biochemical values of thioacetamide (TAA)-injured ICR mice

Treatment		T-triglyceride (mg dL^{-1})	T-cholesterol (mg dL^{-1})	T-bilirubin (mg dL^{-1})	Albumin (g dL^{-1})	AST (U L^{-1})	ALT (U L^{-1})	LDH (U L^{-1})
TAA	Silymarin							
−	−	83.2 ± 5.1a	167.1 ± 5.0a	0.2 ± 0.1a	3.3 ± 0.1a	87.0 ± 11.2b	36.6 ± 7.3b	1186.0 ± 116.6bc
−	+	75.8 ± 6.0a	166.6 ± 7.6a	0.2 ± 0.1a	3.0 ± 0.1a	67.6 ± 6.4b	36.6 ± 9.1b	1068.8 ± 114.4c
+	−	57.4 ± 2.0b	84.2 ± 2.6c	0.2 ± 0.1a	3.2 ± 0.2a	164.8 ± 10.8a	227.4 ± 47.7a	2335.2 ± 365.0b
+	+	83.8 ± 4.3a	118.2 ± 5.2b	0.2 ± 0.1a	3.2 ± 0.1a	90.0 ± 2.9b	67.6 ± 8.9b	1436.8 ± 155.7a

Data are expressed as mean ± standard error of mean ($n = 6$). Mean values of each parameter with different letters are significantly different ($P < 0.05$).
T-triglyceride, total triglyceride; T-cholesterol, total cholesterol; T-bilirubin, total bilirubin; AST, aspartate aminotransferase; ALT, alanine aminotransferase; LDH, lactate dehydrogenase.

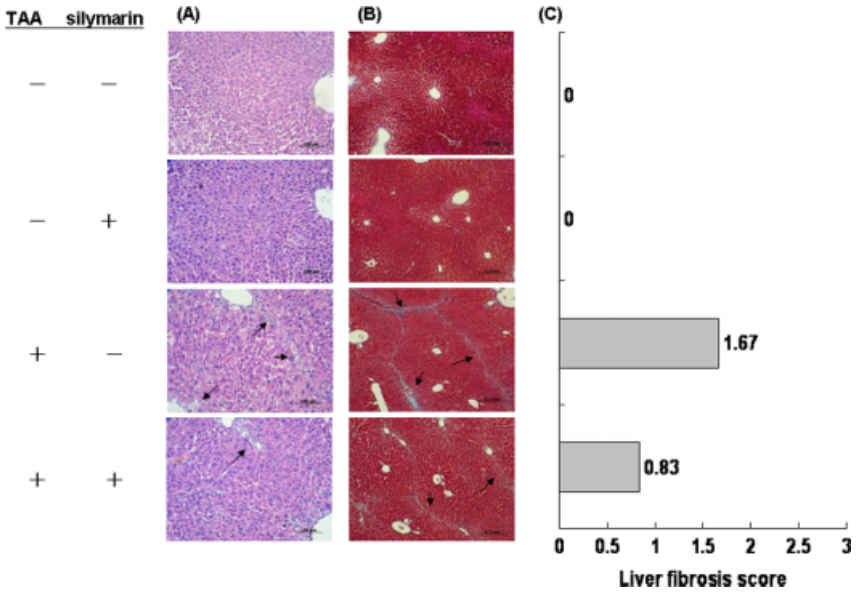

Figure 3. Thioacetamide (TAA) treatment for 8 weeks produced (A) acute focal necrosis and vacuolisation in some liver cells, mild inflammatory cell infiltration and lobular damage (arrows; H&E stain) and (B) collagen deposition between liver lobules (arrows; Masson's Trichrome stain). Co-treatment with silymarin resulted in fewer liver lesions. (C) METAVIR fibrosis scores.

control mice, nor did it affect mRNA levels of genes involved in HSC activation or profibrosis. MMP-2, MMP-13, TIMP-1 and TIMP-2 were up-regulated ($P < 0.05$) in TAA-treated mice, but co-treatment with silymarin reduced MMP-13 and TIMP-1 expression (Fig. 4A). Regarding genes involved in HSC activation and profibrosis, TAA increased NF-κB, AP-1, KLF6, TGF-β1, α-SMA and COL-α1 mRNA levels; however, silymarin partially or completely blocked the up-regulated gene expression, except for NF-κB (Fig. 4(B)).

DISCUSSION

TAA has been shown to increase AST, ALT and LDH levels.[26] In addition, Moreira *et al.*[27] reported that TAA alters fatty acid composition in tissues, thus decreasing fatty acid biosynthesis in the liver and lowering serum T-triglyceride. The lower serum T-triglyceride value caused by TAA treatment is similar to that observed in human liver cirrhosis. Pallottini *et al.*[28] also reported that TAA reduced 3-hydroxy-3-methylglutaryl coenzyme A reductase (HMG-CoA reductase) activity, which may explain the lower serum T-cholesterol level observed in mice treated with TAA (Table 1). Other serum biochemical values did not differ between control and TAA groups, indicating that TAA causes chronic liver damage but not kidney or heart damage. In addition to this biochemical evidence, damage and inflammation in hepatocytes were observed by H&E stain and an apparent development of liver fibrosis was revealed by Masson's Trichrome stain from the histopathology view and the METAVIR fibrosis scores. Taken together, these results showed that 100 mg kg^{-1} TAA applied three times weekly successfully induced chronic liver fibrosis in male ICR mice.

According to a study by Ljubuncic *et al.*,[8] Sprague-Dawley rats treated with TAA had lower body weight and larger liver size compared with untreated rats, which was consistent with the present study. However, the lower body weight in TAA-injured mice differs from most non-alcoholic fatty liver disease models,[29,30] because TAA-induced liver damage is not caused by diet or factors related to obesity. Analysis of serum biochemical values and histopathology revealed that TAA-induced liver damage is very similar to human liver cirrhosis. Silymarin has been shown to protect the liver against increased oxidative stress caused by alcohol consumption[13,31] or CCl_4.[15] Our findings demonstrate that silymarin also protects the liver against TAA-induced damage.

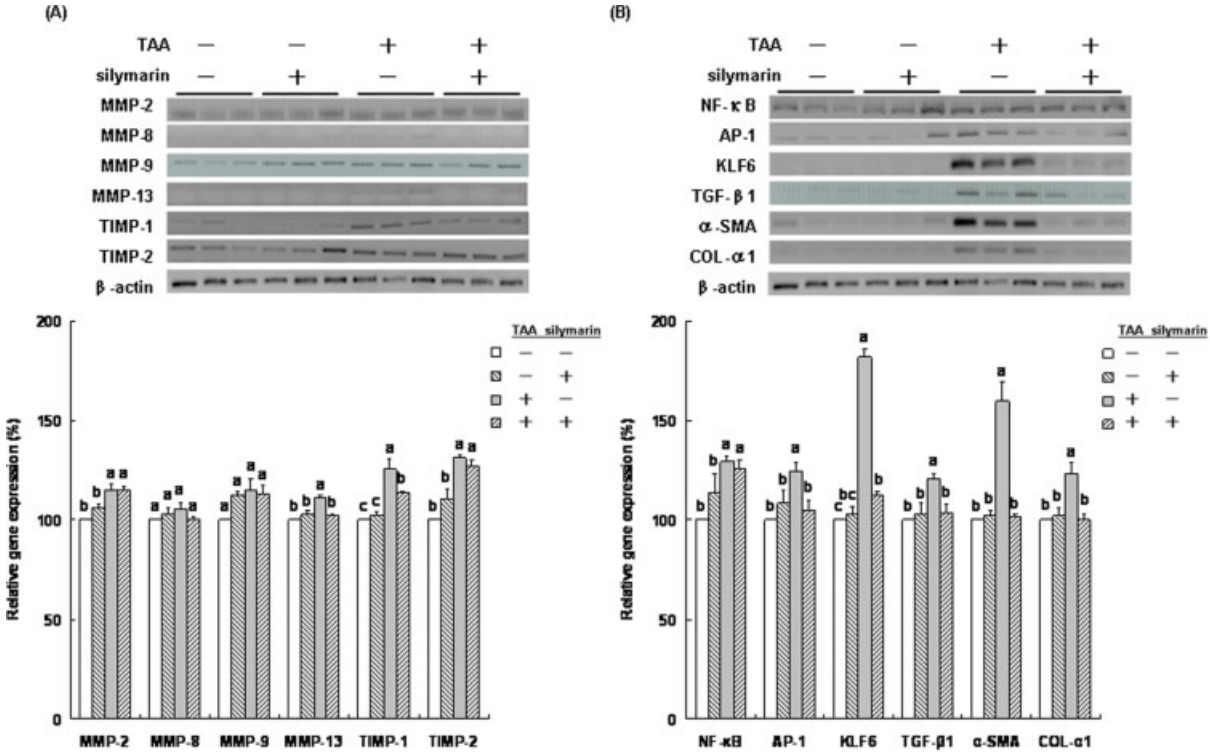

Figure 4. (A) Hepatic MMP and TIMP mRNA levels and (B) hepatic stellate cell activation and profibrosis of thioacetamide (TAA)-injured mice affected by oral gavage of silymarin. Data are expressed as mean ± standard error of mean ($n = 6$). Different letters within each target gene indicate significantly different values ($P < 0.05$). Gene expression was normalised to β-actin and expressed relative to untreated mice.

MMPs are zinc- and calcium-dependent proteases that participate in the degradation of ECM molecules. Major components of the ECM in liver fibrosis include collagen types I, III and IV. MMP-2, MMP-8, MMP-9 and MMP-13 cause fibrinolysis and tissue remodelling, which results in the progression of liver fibrosis.[17] Lichtinghagen *et al*.[18] reported that expression of MMP-2, MMP-7 and MMP-9 as well as TIMP-1 and TIMP-2 is increased in hepatitis C virus-induced end-stage cirrhosis. Increased MMP-13 gene expression was also observed in early-phase liver fibrosis induced by alcohol in rats[32] and in fibrogenesis of cholestatic livers.[33] Activation of HSCs is also regarded as a major cause of liver fibrosis. Recently, Difeo *et al*.[20] reported that KLF6 regulates several profibrogenic genes expressed in activated HSCs, such as TGF-β1 and COL-α1. Previous studies have indicated that higher MMP-2 and MMP-9 activities and HSC activation induced by CCl_4,[34] acetaminophen[35] and high-fat/high-cholesterol diets[29] resulted in liver damage. Hence the TAA-induced liver damage observed in the present study may be due to MMP and TIMP up-regulation and HSC activation (Figs 3 and 4). Protective effects exerted by silymarin against acetaminophen-induced kidney damage[14] and CCl_4-induced liver damage[15] were primarily attributed to reduced lipid peroxidation. Our findings indicate that the hepatoprotective molecular mechanism of silymarin on TAA-induced chronic liver fibrosis involves down-regulation of MMP-2, MMP-13, TIMP-1, TIMP-2, AP-1, KLF6, TGF-β1, α-SMA and COL-α1.

In summary, a mouse model of chronic liver fibrosis was successfully established by injecting 100 mg kg^{-1} TAA three times weekly in male ICR mice; this model was confirmed by serum biochemical and histopathological analyses. Silymarin alone did not alter body weight or liver size or induce liver damage in ICR mice. However, mice treated with TAA had lower body weight and larger livers. In addition, TAA induced chronic liver fibrosis, possibly via up-regulation of MMP-2, MMP-13, TIMP-1, TIMP-2, NF-κB, AP-1, KLF6, TGF-β1, α-SMA and COL-α1. Co-treatment with silymarin exerted hepatoprotective effects against TAA damage. The molecular mechanism of silymarin action may be attributed to suppressing TAA-mediated induction of MMP-2, MMP-13, TIMP-1, TIMP-2, AP-1, KLF6, TGF-β1, α-SMA and COL-α1.

ACKNOWLEDGEMENTS

We would like to acknowledge the funding of this research by the National Science Council, Taiwan (ROC.) (project 98-2313-B-002-021-MY3) and the Department of Health, Executive Yuan, Taiwan (ROC) (project DOH95-TD-HF-111-003).

REFERENCES

1 International Agency for Research on Cancer, World Cancer Report 2008. [Online]. (2009). Available: http://www.iarc.fr/en/publications/pdfs-online/wcr/2008/wcr_2008.pdf [18 December 2008].
2 Department of Health, Executive Yuan, Taiwan, Health Statistics in Taiwan, 2008. [Online]. (2010). Available: http://www.doh.gov.tw/ufile/doc/2008e.xls [6 July 2010].
3 Regimbeau JM, Abdalla EK, Vauthey JN, Lauwers GY, Durand F, Nagorney DM, *et al*, Risk factors for early death due to recurrence after liver resection for hepatocellular carcinoma: results of a multicenter study. *J Surg Oncol* **85**:36–41 (2004).
4 Bataller R and Brenner DA, Liver fibrosis. *J Clin Invest* **115**:209–218 (2005).
5 Childs JFL and Siegler EA, Uses of thioacetamide in agriculture. *Science* **102**:68–72 (1945).
6 Chieli E and Malvaldi G, Role of the microsomal FDA-containing monooxygenase in the liver toxicity of thioacetamide *S*-oxide. *Toxicology* **31**:41–52 (1984).

7 Bruck R, Aeed H, Avni Y, Shirin H, Matas Z, Shahmurov M, *et al*, Melatonin inhibits nuclear factor kappa B activation and oxidative stress and protects against thioacetamide induced liver damage in rats. *J Hepatol* **40**:86–93 (2004).
8 Ljubuncic P, Song H, Cogan U, Azaizeh H and Bomzon A, The effects of aqueous extracts prepared from the leaves of *Pistacia lentiscus* in experimental liver disease. *J Ethnopharmacol* **22**:198–204 (2005).
9 Kang JS, Wanibuchi H, Morimura K, Wongpoomchai R, Chusiri Y, Gonzalez FJ, *et al*, Role of CYP2E1 in thioacetamide-induced mouse hepatotoxicity. *Toxicol Appl Pharmacol* **228**:295–300 (2008).
10 Porter WR and Neal RA, Metabolism of thioacetamide and thioacetamide *S*-oxide by rat liver microsomes. *Drug Metabol Dispos* **6**:379–388 (1978).
11 Hung MY, Fu TY, Shih PH, Lee CP and Yen GC, Du-zhong (*Eucommia ulmoides* Oliv.) leaves inhibit CCl_4-induced hepatic damage in rats. *Food Chem Toxicol* **44**:1424–1431 (2006).
12 Wu JW, Lin LC and Tsai TH, Drug–drug interactions of silymarin on the perspective of pharmacokinetics. *J Ethnopharmacol* **121**:185–193 (2009).
13 Saller R, Meier R and Brignoli R, The use of silymarin in the treatment of liver diseases. *Drugs* **61**:2035–2063 (2001).
14 Sonnenbichler J, Scalera F, Sonnenbichler I and Weyhenmeyer R, Stimulatory effects of silibinin and silicristin from the milk thistle *Silybum marianum* on kidney cells. *J Pharmacol Exp Therapeut* **290**:1375–1383 (1999).
15 Lettéron P, Labbe G, Degott C, Berson A, Fromenty B, Delaforge M, *et al*, Mechanism for the protective effects of silymarin against carbon tetrachloride-induced lipid peroxidation and hepatotoxicity in mice: evidence that silymarin acts both as an inhibitor of metabolic activation and as a chain-breaking antioxidant. *Biochem Pharmacol* **39**:2027–2034 (1990).
16 Visse R and Nagase H, Matrix metalloproteinases and tissue inhibitors of metalloproteinases: structure, function, and biochemistry. *Circ Res* **92**:827–839 (2003).
17 Consolo M, Amoroso A, Spandidos DA and Mazzarino MC, Matrix metalloproteinases and their inhibitors as markers of inflammation and fibrosis in chronic liver disease. *Int J Mol Med* **24**:143–152 (2009).
18 Lichtinghagen R, Michels D, Haberkorn CI, Arndt B, Bahr M, Flemming P, *et al*, Matrix metalloproteinase (MMP)-2, MMP-7, and tissue inhibitor of metalloproteinase-1 are closely related to the fibroproliferative process in the liver during chronic hepatitis C. *J Hepatol* **34**:239–247 (2001).
19 Mann DA and Smart DE, Transcriptional regulation of hepatic stellate cell activation. *Gut* **50**:891–896 (2002).
20 Difeo A, Martignetti JA and Narla G, The role of KLF6 and its splice variants in cancer therapy. *Drug Resist Updates* **12**:1–7 (2009).
21 Chia R, Achilli F, Festing MFW and Fisher EMC, The origins and uses of mouse outbred stocks. *Nat Genet* **37**:1181–1186 (2005).
22 Hung KS, Lee TH, Chou WY, Wu CL, Cho CL, Lu CN, *et al*, Interleukin-10 gene therapy reverses thioacetamide-induced liver fibrosis in mice. *Biochem Biophys Res Commun* **336**:324–331 (2005).
23 Yang JI, Yoon JH, Bang YJ, Lee SH, Lee SM, Byun HJ, *et al*, Synergistic antifibrotic efficacy of statin and protein kinase C inhibitor in hepatic fibrosis. *Am J Physiol Gastrointest Liver Physiol* **298**:G126–G132 (2010).
24 Popov Y, Sverdlov DY, Sharma AK, Bhaskar KR, Li S, Freitag TL, *et al*, Tissue transglutaminase does not affect fibrotic matrix stability or regression of liver fibrosis in mice. *Gastroenterology* **140**:1642–1652 (2011).
25 Brunt EM, Grading and staging the histological lesions of chronic hepatitis: the Knodell histology activity index and beyond. *Hepatology* **31**:241–246 (2000).
26 Túnez I, Muñoz MC, Villavicencio MA, Medina FJ, de Prado EP, Espejo I, *et al*, Hepato- and neurotoxicity induced by thioacetamide: protective effects of melatonin and dimethylsulfoxide. *Pharmacol Res* **52**:223–228 (2005).
27 Moreira E, Fontana L, Periago JL, Sanchéz De Medina F and Gil A, Changes in fatty acid composition of plasma, liver microsomes, and erythrocytes in liver cirrhosis induced by oral intake of thioacetamide in rats. *Hepatology* **21**:199–206 (1995).
28 Pallottini V, Martini C, Bassi AM, Romano P, Nanni G and Trentalance A, Rat HMGCoA reductase activation in thioacetamide-induced liver injury is related to an increased reactive oxygen species content. *J Hepatol* **44**:368–374 (2006).
29 Yang SF, Tseng JK, Chang YY and Chen YC, Flaxseed oil attenuates nonalcoholic fatty liver of hyperlipidemic hamsters. *J Agric Food Chem* **57**:5078–5083 (2009).
30 Yang DJ, Chang YY, Hsu CL, Liu CW, Lin YL, Lin YH, *et al*, Antiobesity and hypolipidemic effects of longan (*Dimocarpus longans* Lour.)-flower-water-extract in hypercaloric-dietary rats. *J Agric Food Chem* **58**:2020–2027 (2010).
31 Huang CH, Chang YY, Kang WY, Lin YL, Chang HC and Chen YC, Fruiting body of Niuchangchih (*Antrodia camphorata*) protects livers against chronic alcohol-consumption damage. *J Agric Food Chem* **58**:3859–3866 (2010).
32 Yan S, Chen GM, Yu CH, Zhu GF, Li YM and Zheng SS, Expression pattern of matrix metalloproteinases-13 in a rat model of alcoholic liver fibrosis. *Hepatobiliary Pancreat Dis Int* **4**:569–572 (2005).
33 Uchinami H, Seki E, Brenner DA and D'Armiento J, Loss of MMP 13 attenuates murine hepatic injury and fibrosis during cholestasis. *Hepatology* **44**:420–429 (2006).
34 Shyu MH, Kao TC and Yen GC, Hsian-tsao (*Mesona procumbens* Heml.) prevents against rat liver fibrosis induced by CCl_4 via inhibition of hepatic stellate cells activation. *Food Chem Toxicol* **46**:3707–3713 (2008).
35 Ito Y, Abril ER, Bethea NW and McCuskey RS, Inhibition of matrix metalloproteinases minimizes hepatic microvascular injury in response to acetaminophen in mice. *Toxicol Sci* **83**:190–196 (2005).

